

Extragalactic maser surveys

C. Henkel^{1,2}, J.-E. Greene³ and F. Kamali¹

¹Max-Planck-Institut für Radioastronomie, Auf dem Hügel 60, 53121 Bonn, Germany

²Astron. Dept., King Abdulaziz University, P.O. Box 80203, Jeddah 21589, Saudi Arabia

³Department of Astrophysical Sciences, Princeton University, Princeton, NJ 08544, USA
email: chenkel@mpifr-bonn.mpg.de

Abstract. Since the IAU (maser-)Symposium 287 in Stellenbosch/South Africa (Jan. 2012), great progress has been achieved in studying extragalactic maser sources. Sensitivity has reached a level allowing for dedicated maser surveys of extragalactic objects. These included, during the last years, water vapor (H₂O), methanol (CH₃OH), and formaldehyde (H₂CO), while surveys related to hydroxyl (OH), cyanoacetylene (HC₃N) and ammonia (NH₃) may soon become (again) relevant. Overall, with the upgraded Very Large Array (VLA), the Atacama Large Millimeter/submillimeter Array (ALMA), FAST (Five hundred meter Aperture Synthesis Telescope) and the low frequency arrays APERTIF (APERTure Tile in Focus), ASKAP (Australian Square Kilometer Array Pathfinder) and MeerKAT (Meer Karoo Array Telescope), extragalactic maser studies are expected to flourish during the upcoming years. The following article provides a brief sketch of past achievements, ongoing projects and future perspectives.

Keywords. masers, galaxies: active, galaxies: ISM, galaxies: Seyfert, radio lines: galaxies

1. The past few decades

Maser lines allow us to detect and to localize tiny hotspots with exceptional activity across the Universe. These can be used to highlight regions with enhanced star formation, allow for determinations of proper motion out to distances of several Mpc, and help us to constrain the morphology and distance of galaxies. Before addressing recent or ongoing extragalactic maser surveys, here we briefly summarize achievements obtained till the time of the Stellenbosch meeting. We then proceed with the Local Group of galaxies (Sect. 2), H₂O megamaser projects (Sects. 3–6), the search for a correlation between H₂O and OH megamasers (Sect. 7), formaldehyde (Sect. 8), methanol, HC₃N, and HCN (Sect. 9), and future perspectives (Sect. 10).

Extragalactic 1.7 GHz (18 cm) OH masers were detected as early as in the mid seventies (e.g., Gardner & Whiteoak 1975), soon followed by the detection of a bright 22 GHz H₂O maser in M 33 by Churchwell et al. (1977). While line luminosities were high by Galactic standards, they were not surpassing their more local cousins by many orders of magnitude. This drastically changed, when the first “megamasers” were detected, this time in opposite order, starting with 22 GHz H₂O in NGC 4945 (Dos Santos & Lepine 1979) and followed by 1.7 GHz OH in Arp 220 (Baan et al. 1982). During the following years the interest mainly focused on OH, because these megamasers were rapidly associated with a so far not well known class of galaxies, the ULIRGs (UltraLuminous InfraRed Galaxies). This culminated in the large survey carried out by Darling & Giovanelli (2002), leading to a total number of ≈ 100 detected OH megamaser sources. With respect to 22 GHz H₂O megamasers, it took more than 15 years until it became clearer what they represented and in which class of galaxies they could be found. However, even today detection rates are typically below 10%. Crucial discoveries were the detection of satellite lines well off the systemic velocity in NGC 4258 (Nakai et al. 1993), the discov-

ery of velocity drifts of the near systemic maser components of NGC 4258 (Haschick et al. 1994; Greenhill et al. 1995), the mapping of the H₂O maser features in NGC 4258 (Miyoshi et al. 1995), and the discovery that 22 GHz H₂O masers are most commonly found in Seyfert 2 and LINER (Low Ionization Nuclear Emission Line Region) galaxies (Braatz et al. 1996, 1997). All this indicated that some of the luminous water vapor masers, the so-called disk-masers, are forming Keplerian parsec or even sub-parsec scale accretion disks around their galaxy’s supermassive nuclear engines, allowing for a determination of the disk’s geometry, the mass of the nuclear engine, and the angular diameter distance to the parent galaxy.

Another molecular transition, the 4.8 GHz $J = 1$ K-doublet line of formaldehyde (H₂CO). was also proposed to be masing, greatly surpassing any Galactic counterpart in luminosity, Commonly seen in absorption, quasi-thermal 4.8 GHz emission lines form at densities of at least several 10^5 cm^{-3} , while maser emission is rarely seen in the Galaxy (e.g., Ginsburg et al. 2015). 4.8 GHz H₂CO emission was detected toward Arp 220, IC 680, and IR 15107+0724 (Baan et al. 1986; Baan et al. 1993; Araya et al. 2004) and, in the initial paper, the line from Arp 220 was interpreted as a maser likely amplifying the non-thermal radio background of the source.

2. The Local Group

The Large and Small Magellanic Clouds (LMC and SMC) allow for studies of masers commonly observed in the Galaxy, but under conditions of low metallicity and strong UV-radiation fields. During the past few years, Breen et al. (2013), Imai et al. (2013), and Johanson et al. (2014), mainly using the Australia Compact Array (ATCA), were successful in finding new maser spots related to star formation. In the LMC, now we have 27 H₂O masers originating from 15 regions of star formation, and 3 such masers from late type stars. With the study of Breen et al. (2013), four new 22 GHz H₂O masers were detected in the SMC, thus tripling the number obtained three decades before by Scalise & Braz (1982). Most of these sources can greatly help, through proper motion measurements, to constrain the individual rotation of the two galaxies as well as to measure their orbital motion around the Milky Way.

Proper motion is also the main motivation to systematically measure the less conspicuous members of the Local Group at 6.7 and 22 GHz, searching for methanol and water vapor masers using the Sardinia Radio Telescope (SRT). Results from this ongoing project are summarized by the contribution of A. Tarchi.

In the Andromeda galaxy (M 31) Sjouwerman et al. (2010) and Darling (2011) detected first 6.7 GHz CH₃OH and 22 GHz H₂O masers, respectively. After this encouraging start, however, no new maser sources could be identified during the following years (see Darling et al. 2016, who surveyed ≈ 500 additional sources with compact 24 μm emission in M 31). The unknown proper motion of M 31 is the main obstacle on the way to a basic understanding of Local Group dynamics. Therefore, detecting many such maser lines with suitable flux density for interferometric studies is of high importance.

3. H₂O megamaser detection surveys

Already before the Stellenbosch meeting, dedicated 22 GHz H₂O maser surveys have been carried out. These include unsuccessful searches for Fanaroff-Riley I (FR I) galaxies (Henkel et al. 1998) and relatively nearby low luminosity type I and type II QSOs (Bennert et al. 2009; König et al. 2012) as well as the detection of maser emission in an FR II galaxy (Tarchi et al. 2003). Additional surveys lead to the detection of a type 2 QSO at

redshift $z = 0.66$ (Barvainis & Antonucci 2005) and to the detection of a gravitationally lensed type I QSO at $z = 2.64$ (Impellizzeri et al. 2008; Castangia et al. 2011; McKean et al. 2011).

Searching for 22 GHz H_2O masers mainly toward Narrow-Line Seyfert 1 galaxies (NLS1s), which appear to contain relatively low mass nuclear engines but luminosities compatible with their broad-line counterparts, Tarchi et al. (2011) reported two new detections, thus leading to a total of five known masers in this type of galaxies. The more recent survey by Hagiwara et al. (2013a) did not yield new positive results.

Another survey lacking new detections, but also with high relevance for our understanding of the H_2O megamaser phenomenon and the calibration of nuclear mass determinations, has been carried out by van den Bosch et al. (2016). They observed galaxies, where the gravitational sphere of influence of the central engine is extended enough to be resolvable by present day optical or near infrared (NIR) facilities. The detection of H_2O disk-masers in such galaxies would have a great impact. The radio data would provide a reliable black hole mass, which could then be compared with those derived by other potentially less accurate methods using optical or NIR data. The non-detections imply that NGC 4258 was and still remains the only such calibrator, where nuclear masses derived from H_2O and other methods, applicable to a larger number of galaxies, could be compared. Furthermore, most galaxies observed by van den Bosch et al. (2016) were of early type, with estimated nuclear masses $M_{\text{BH}} \gtrsim 10^8 M_{\odot}$. Apparently, there is a rather

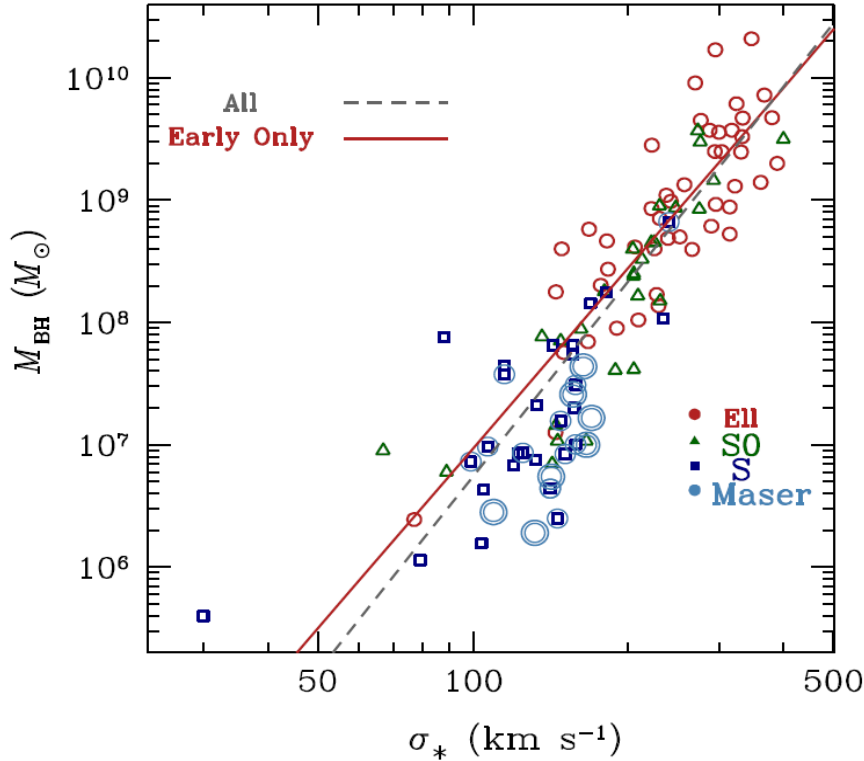


Figure 1. Relationship between stellar velocity dispersion and central mass (M_{BH} , taken from Greene et al. 2016). Dashed line: Fit to the entire sample. Solid line: Early type galaxies only. Small open circles: ellipticals; small open triangles: lenticulars; small open squares: spirals; single circles surrounding an open square or double circles: disk-maser galaxies.

narrow window for the occurrence of H₂O megamasers, which appear to be confined to nuclear regions with $10^6 M_{\odot} < M_{\text{BH}} < 10^8 M_{\odot}$.

There are also recent 22 GHz H₂O surveys with detections. Beside the RadioAstron measurements of known sources with ultrahigh angular resolution, discussed by W. A. Baan in this volume, a single-dish study to be mentioned in this context is that of Wagner (2013). He targeted Seyfert 2 galaxies with high X-ray luminosity and high hydrogen column density, also including a few OH-absorbers. His detection rate, 4 out of 37 galaxies, exceeds 10% and therefore provides a good example on how to select promising sources. Yamauchi et al. (2017) chose galaxies with an absorbed 2 keV continuum, a strong Fe 6.4 keV line and significant infrared emission. They detected three galaxies in a sample of 10 targets, an exceptionally high detection rate, with the caveat that their sample is comparatively small. Finally, Zhang et al. (2012) and Liu et al. (2017) showed that almost exclusively Seyfert 2 galaxies with high radio continuum luminosities are exhibiting H₂O maser emission. This led to a successful pilot study involving 18 sources (see Zhang et al. 2017) and the contribution by J.S. Zhang in this volume.

4. The MCP

At the core of the present extragalactic 22 GHz H₂O maser research stands the Megamaser Cosmology Project (MCP) with the goals (1) to study accretion disk morphology, (2) to determine nuclear black hole masses, and (3) to constrain the Hubble constant to a precision of a few percent, avoiding any standard candles but using instead a direct geometric approach (see Herrstein et al. 1999 for the first application of this technique). Introduced at the Stellenbosch meeting by Henkel et al. (2012), three MCP articles had been published by that time, two on UGC 3789 and one on black hole masses (Reid et al. 2009; Braatz et al. 2010; Kuo et al. 2011). In addition, Greene et al. (2010) analyzed obtained black hole masses as a function of associated bulge masses. More recently, the number of MCP publications has tripled (Reid et al. 2013, Kuo et al. 2013, 2015, Pesce et al. 2015, Gao et al. 2016, 2017). These articles present detailed high resolution maps of a total of nine galaxies, most of them exhibiting the common disk-maser fingerprint. Detailed results are presented by J. A. Braatz, in this volume. In addition, maser disk physics and upper magnetic field limits were discussed. Following Pesce et al. (2015), the spiral shock model proposed by Maoz & McKee (1998) is not consistent with the measured properties of the maser disks, since the so-called high velocity features, hundreds of km s^{-1} off the parent galaxy's systemic velocity, do not show any of the predicted systematic velocity drifts. Limits obtained searching for Zeeman splitting typically reach 200-300 mG (1σ), while the corresponding limit for NGC 1194 is 73 mG.

Beside disk morphology, M_{BH} , and geometric distance, there are three major lines of research making use of the data supplied by the MCP: (1) A comparison of the resulting supermassive black hole masses with those derived by gas or stellar dynamics, bulge mass, total galactic mass, or mass within the central kiloparsec; (2) a comparison of position angle and inclination of the respective galaxies as a function of radius, starting from the outer large scale disk and proceeding to the smallest scales, provided by the H₂O disk-masers, representing a nuclear disk viewed edge-on; (3) a test of the AGN paradigm, involving a supermassive nuclear engine, a jet, and, perpendicular to it, an accretion disk.

(1) Comparisons of the mass of the nuclear engine with those of other galactic parameters reveal poor correlations, thus leading to results which drastically differ from the tight correlation obtained for massive elliptical galaxies. Furthermore it appears (see Fig. 1) that the masses of the supermassive nuclear engines of megamaser galaxies are below the expected correlation, while similarly sized spiral galaxies studied at optical or NIR

wavelengths do not show this effect. Greene et al. (2016) and Läscher et al. (2016)) offer two most likely explanations for this effect: Either the non-maser selected galaxies miss the low mass end of the BH distribution due to an inability to resolve their spheres of influence or the disk-maser galaxies preferentially occur in lower BH-mass environments.

(2) The disk-maser galaxies with their known nuclear morphology allow for a unique comparison of position angles between largest and smallest scales. This reveals that the megamaser disks are neither aligned with the large scale disks of their parent galaxies nor with the morphology encountered at a galactocentric radius close to 100 pc (Greene et al. 2010, 2013; Pjanka et al. 2016). Fig. 2 shows correlations between the large and $r \approx 200$ pc scale (left panels) and between the $r \approx 200$ pc and ≈ 1 pc disk maser orientations. A differentiation between $r > 200$ pc and < 200 pc is also presented (lower panels).

(3) To become detectable, the 22 GHz H_2O maser line requires gas fulfilling certain boundary conditions, like kinetic temperatures $T_{\text{kin}} \gtrsim 300$ K and very high densities, $n(\text{H}_2) \gtrsim 10^7 \text{ cm}^{-3}$ (e.g., Kylafis & Norman 1991). Thus, the H_2O line is confined to a specific physical environment and is certainly not telling the entire story. To gain deeper insights, radio continuum data are an excellent additional probe because they can be obtained with similar angular resolution and are also not affected by dust extinction. With the geometry being known, i.e. with nuclear disks viewed edge-on, radio continuum data are ideal to check the AGN paradigm: Are there jets and are these really two-sided, as it is expected for jets ejected parallel to the plane of the sky? Can we follow individual

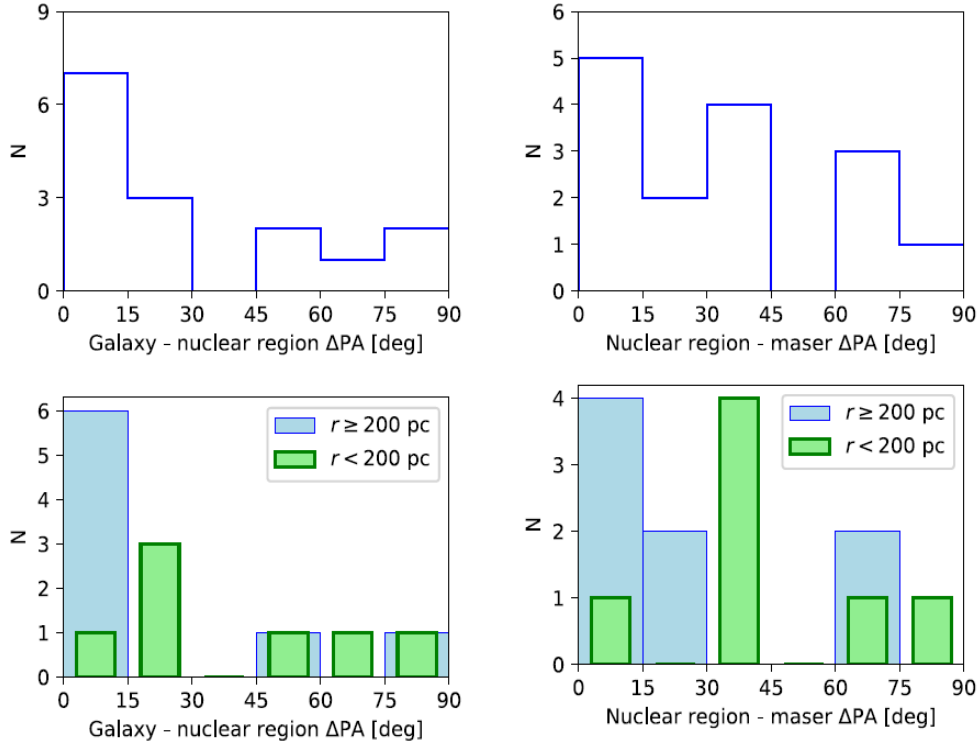


Figure 2. Position angle (PA) differences between the angular momenta of the large scale disk versus the central region at radius $r \approx 200$ pc (left) and the central region versus the pc-scale megamaser disk (right). The two lower panels also differentiate between nuclear regions $r < 200$ pc and > 200 pc, still indicating a possible alignment between the large scale disks and the $r > 200$ pc regions, but not with the $r < 200$ pc environment. Only the smaller one of two possible position angles is shown (the other one is 180° minus the given angle).

blobs, thus directly determining their speed? Can we detect emission from inside the maser disks? And are there correlations with the nuclear mass and/or the size of the maser disks? With this motivation dedicated continuum measurements at 33 GHz (Very Large Array, VLA) and 5 GHz (Very Long Baseline Array, VLBA) have been carried out. Some preliminary VLBA results related to this ongoing project are presented by F. Kamali in this volume. Fig. 3 shows the correlations between the 33 GHz VLA continuum flux densities and the inner and outer maser disk radii.

5. A caveat when analyzing 22 GHz H₂O maser emission

Arp 220 with its extreme infrared luminosity ($L_{\text{IR}} \gtrsim 10^{12} L_{\odot}$) is often taken as the prototypical ULIRG. With the characteristic ratio of 10^{-9} between (isotropic) 22 GHz H₂O and infrared luminosity (e.g., fig. 9 in Henkel et al. 2005), we could thus expect strong maser emission with $L_{\text{H}_2\text{O}} \approx 1000 L_{\odot}$, yielding a flux density of ≈ 20 mJy, if evenly distributed over a velocity range of 400 km s^{-1} . Even in case of a deviation from this rule by a full factor of ten, 22 GHz H₂O maser lines are characterized by narrow spikes (e.g., Fig. 4), which would likely compensate for this effect. Furthermore, Arp 220 is characterized by a star formation rate amounting to a few $100 M_{\odot} \text{ yr}^{-1}$ (e.g., Kennicutt 1998). Therefore there should be many star formation related H₂O masers, so many, that deviations from the 10^{-9} -rule might be minimized. In this respect it is noteworthy that 22 GHz maser emission from this merging galaxy pair has only been detected recently (Zschaechner et al. 2016). The reason is absorption by the NH₃ (J, K) = (3,1) transition. The NH₃ (3,1) line at 22.234506 GHz with levels 165 K above the ground state and the H₂O line at 22.235080 GHz, 645 K above the ground state, are separated by only $\Delta V \approx 8 \text{ km s}^{-1}$. Zschaechner et al. (2016) find approximately -60 Jy km s^{-1} for the western and $+60 \text{ Jy km s}^{-1}$ for the eastern nucleus of Arp 220 (the absolute values are the same within $\approx 5\%$), thus canceling but a negligible fraction of the total signal if viewed by a single-dish telescope. Toward the western nucleus NH₃ absorption dominates, while toward the eastern one emission, likely due to H₂O, is mainly seen. Apparently, when observing ULIRGs, high resolution data are mandatory, because in such galaxies gas densities and

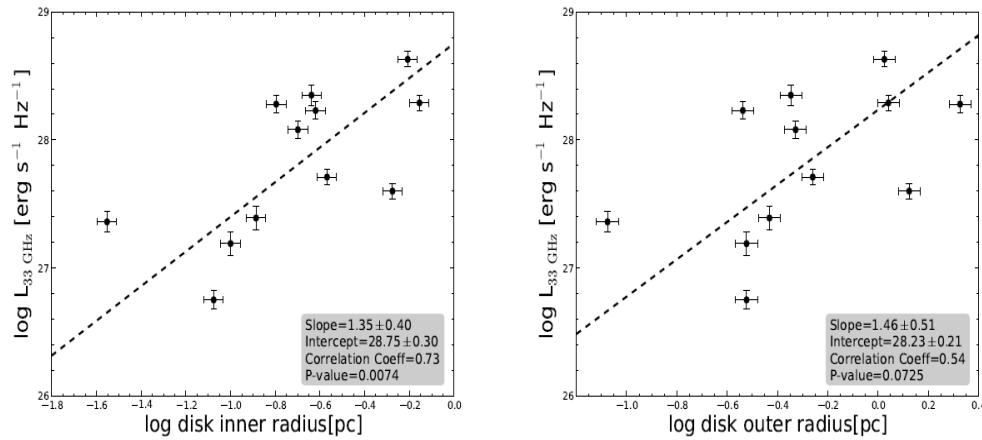


Figure 3. Maser disk inner (left) and outer (right) radius versus VLA 33 GHz continuum luminosity. Slope, intercept, correlation coefficient and p-values (likelihood that there is no correlation) are also given. From Kamali et al. (2017).

kinetic temperatures tend to be high, thus providing suitable conditions for the presence of non-metastable ammonia transitions interfering with the 22 GHz maser emission from H_2O if there is a continuum which can be absorbed. For an evaluation of the intensity of the NH_3 (3,1) line, then the detection of other non-metastable cm-wave NH_3 inversion transitions will be mandatory.

6. Other H_2O maser lines

With the 22 GHz H_2O line detected in 178 galaxies (see the contribution by J. Braatz), there are also other promising lines to be observed. Humphreys et al. (2005) (NGC 3079) and Cernicharo et al. 2006 (Arp 220) opened this field by observing the 183 GHz $3_{13} \rightarrow 2_{20}$ transition which is unlike the $6_{16} \rightarrow 5_{23}$ transition at 22 GHz not connecting states 645 K, but levels only 200 K above the ground state. Thus emission is expected to be more widespread than at 22 GHz, but is also affected by atmospheric obscuration, so that a non-zero redshift helps to enhance sensitivity. In recent years several additional studies have been carried out (Hagiwara et al. 2013b, 2016; Galametz et al. 2016, Humphreys et al. 2016, Pesce et al. 2016), focussing on this 183 GHz line but also on the 321 GHz $10_{29} \rightarrow 9_{36}$ transition, ≈ 1850 K above the ground state and thus only tracing extremely highly excited gas. Studied sources (see also the contribution by D. Pesce in this volume) are the Circinus galaxy, where the 321 GHz line is covering a similar velocity range as the 22 GHz line (perhaps even a slightly wider one, see Fig. 4), and NGC 4945, where the 183 GHz line is covering the entire velocity range, while the higher excitation gas sampled by the 321 GHz transitions is only seen at the upper end of the galaxy's velocity

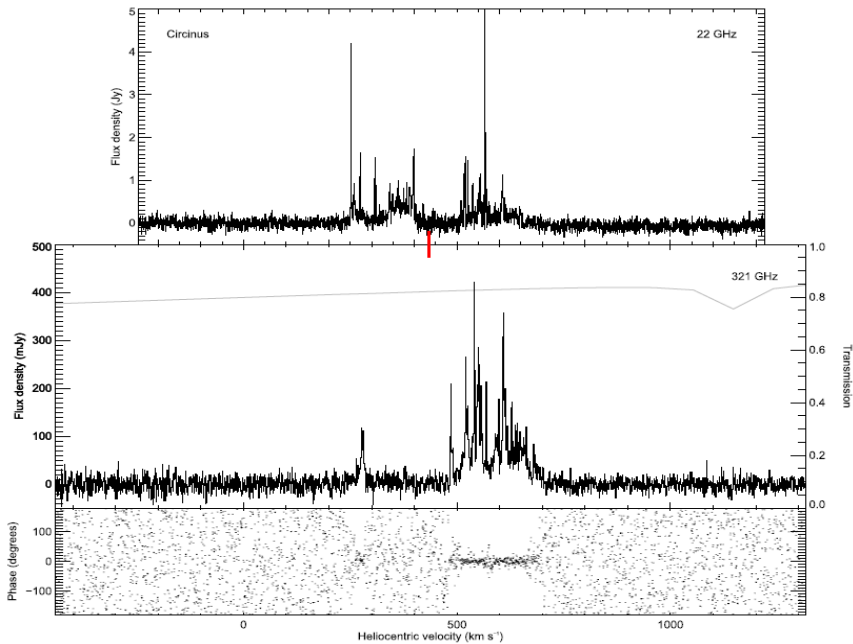


Figure 4. 22 GHz (upper panel) and 321 GHz (lower panel) H_2O maser spectra from the Circinus galaxy. The bottom panel provides a phase plot for the calibrated 321 GHz spectrum. The short vertical line connecting upper and lower panel denotes the systemic velocity. From Pesce et al. (2016)

range, near $V \approx 700 \text{ km s}^{-1}$. What is still missing here are high resolution observations of these lines allowing for a detailed comparison with the 22 GHz data.

7. 1.7 GHz OH versus 22 GHz H₂O

OH and H₂O megamasers appear to be mutually exclusive, likely because they trace very different physical environments. Wiggins et al. (2016) searched with the Green Bank Telescope (GBT) for luminous H₂O maser emission in OH megamaser galaxies and confirmed, after IC 694, with II Zw 96 a second such object. Measuring instead OH in galaxies with strong H₂O masers using the Effelsberg telescope and the GBT, two of the sample galaxies were detected in OH, but in absorption. Details of this latter survey can be found in the contribution by E. Ladu, in this volume.

8. Formaldehyde (H₂CO)

Mangum et al. (2008, 2013) observed, with the Green Bank 100-m telescope, 56 star forming galaxies in the 4.8 and 14.5 GHz K-doublet transitions of formaldehyde (H₂CO). Both transitions were detected in 13 targets, mostly in absorption but sometimes also in emission. Applying Occam's Razor and assuming quasi-thermal and not maser radiation in case of the emission lines, all data could be nicely fitted with a Large Velocity Gradient model, yielding densities in the range $10^{4.5 \dots 5.5} \text{ cm}^{-3}$. Nevertheless, high resolution data from three galaxies with emission lines indicate that brightness temperatures can greatly exceed in some regions those expected in case of thermal emission, reaching values of $10^{4 \dots 5} \text{ K}$ (Baan et al. 2017). The three galaxies are IC 860, IR 15107+0724 and Arp 220 (see Fig. 5 for an image). As a consequence, it would be interesting to evaluate in how far

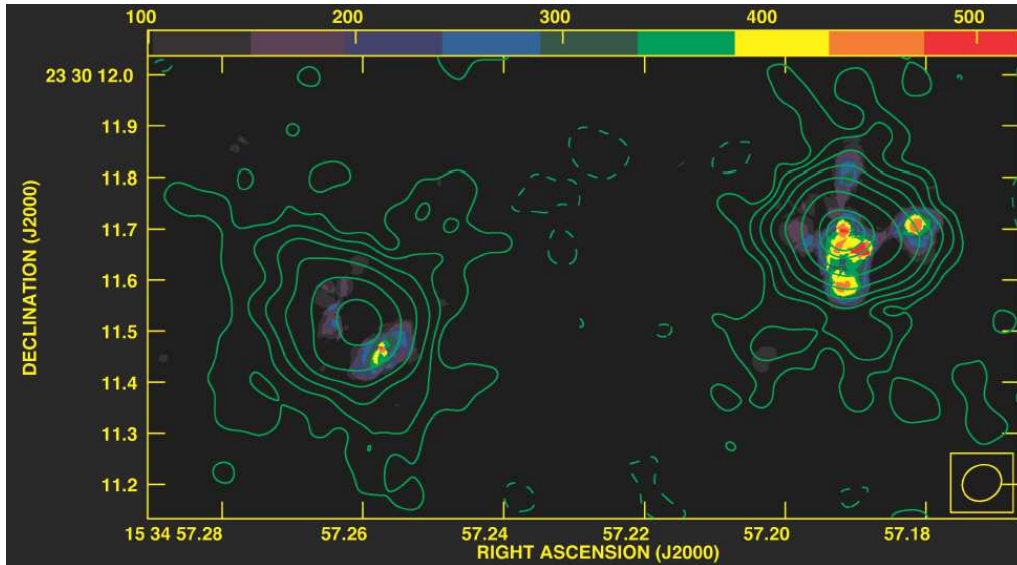


Figure 5. A composite map of the continuum (contours) and the 4.8 GHz formaldehyde emission of Arp 220 (from Baan et al. 2017). Contour levels are $0.3 \times (-1, 1, 2, 4, 8, 16, 32, 64, \text{ and } 80) \text{ mJy beam}^{-1}$ with peak flux densities of ~ 13 and 30 mJy beam^{-1} for the eastern and western nucleus, respectively. A temperature scale in units of $\text{mJy km s}^{-1} \text{ beam}^{-1}$ for the line emission is given at the upper edge of the image. The synthesized beam is indicated in the lower right.

this affects the analysis by Mangum et al. (2080, 2013), which is mainly but not entirely based on H₂CO 4.8 and 14.5 GHz absorption lines.

9. Methanol, HC₃N, and HCN

In the Galaxy, the so-called Class II 6.7 GHz transition exhibits the strongest methanol maser lines, being directly associated with sites of massive star formation (e.g., Menten 1991). Searches for this line in extragalactic space were, however, not very successful, only providing maser detections in the Magellanic Clouds and the Andromeda galaxy (see Sect. 2). After unsuccessfully searching for Class II lines much stronger than those encountered in the Galaxy, Class I masers, being clearly less conspicuous in the Galaxy and less directly associated with sites of massive star formation, have become part of a recent survey. And here, surprisingly, emission much more luminous than the corresponding Galactic masers could be found (Ellingsen et al. 2014, 2017a; Chen et al. 2015, 2016; McCarthy et al. 2017). What makes these detections peculiar is that the masers are not associated with the very center of their parent galaxies, but are instead detected in the outskirts of their nuclear environments. A detailed account of these new findings, including the possible detection of an HC₃N $J = 4 \rightarrow 3$ maser (Ellingsen et al. 2017b), is given by the contributions of S. Ellingsen, X. Chen, and T. McCarthy in this volume. The presence of a weakly masing HCN $J = 1 \rightarrow 0$ line right at the center of the whirlpool galaxy M 51, in a region with relatively weak CO emission, has been proposed by Matsushita et al. (2015).

10. The bright future

Interestingly, and possibly for the first time in this series of meetings, extragalactic OH was not a topic of much discussion. However, this will likely change in the forthcoming years. With Apertif (Aperture Tile in Focus), MeerKat (Meer Karoo Array Telescope), ASKAP (Australia Square Kilometer Array Pathfinder) and FAST (Five hundred meter Aperture Spherical Telescope), new OH surveys sometimes piggybacking on HI measurements, will cover significant parts of the sky. This will greatly help in obtaining new detections of luminous OH masers and to reach eventually an independent estimate of the number of merger galaxies as a function of redshift.

With the Very Large Array (VLA) and possibly also with the Atacama Large Millimeter/submillimeter Array (ALMA), new extragalactic Class I methanol maser surveys can be carried out. Here we are still near the start. While the standard lines near 36 and 44 GHz have been measured in a small number of galaxies, higher frequency Class I masers detectable with ALMA have, to our knowledge, not even been touched.

With respect to 22 GHz H₂O masers, we note that the MCP is close to completion. We can expect a final Hubble constant deduced from this survey with an uncertainty of only a few percent during the next one or two years. However, this will be by no means the end of H₂O megamaser research. Not only other H₂O lines are and will remain attractive. The 22 GHz maser line itself may remain at the center of interest. The reason is that detection rates of future 22 GHz maser surveys have the potential to go up dramatically. So far, average detection rates are well below 10%. Detection rates of disk-masers are even close to or less than 1%. All this may change with the introduction of new criteria, either led by X-ray spectroscopy, by the radio continuum luminosity, or by a combination of the two methods. At the same time, the James Webb Space Telescope (JWST), ALMA and NOEMA (NORthern Extended Millimeter Array) may provide new constraints to the masses of nuclear engines, to be compared with those deduced from the maser-disk data.

References

- Araya, E., Baan, W. A., & Hofner, P. 2004, *ApJS*, 154, 541
- Baan, W. A., Wood, P. A. D., & Haschick, A. D. 1982 *ApJ*, 260, L49
- Baan, W. A., Güsten, R., & Haschick, A. D. 1986, *ApJ*, 305, 830
- Baan, W. A., Haschick, A. D., & Uglesich, R. 1993, *ApJ*, 415, 140
- Baan, W. A., An, T., Klöckner, H.-R., & Thomasson, P. 2017, *MNRAS*, 469, 916
- Barvainis, R., & Antonucci, R. 2005, *ApJ*, 628, L89
- Bennert, N., Barvainis, R., Henkel, C., & Antonucci, R. 2009, *ApJ*, 695, 276
- Braatz, J. A., Wilson, A. S., & Henkel, C. 1996, *ApJS*, 106, 51
- Braatz, J. A., Wilson, A. S., & Henkel, C. 1997, *ApJS*, 110, 321
- Braatz, J. A., Reid, M. J., Humphreys, E. M. L., et al. 2010, *ApJ*, 718, 657
- Breen, S. L., Lovell, J. E. J., Ellingsen, S. P., et al. 2013, *MNRAS*, 432, 1382
- Castangia, P., Impellizzeri, C. M. V., McKean, J. P., et al. 2011, *A&A*, 529, A150
- Cernicharo, J., Pardo, J. R., & Weiß, A. 2006, *ApJ*, 646, L49
- Chen, X., Ellingsen, S. P., Baan, W. A., et al. 2015, *ApJ*, 800, L2
- Chen, X., Ellingsen, S. P., Zhang, J. S., et al. 2016, *MNRAS*, 459, 357
- Churchwell, E., Witzel, A., Huchtmeier, W., et al. 1977, *A&A*, 54, 969
- Darling, J. 2011, *ApJ*, 732, L2
- Darling, J., & Giovanelli, R. 2002, *AJ*, 124, 100
- Darling, J., Gerard, B., Amiri, N., & Lawrence, K. 2016, *ApJ*, 826, 24
- Dos Santos, P. M., & Lepine, J. R. D. 1979, *Nature*, 278, 34
- Ellingsen, S. P., Chen, X., Qiao, H.-H., et al. 2014, *ApJ*, 790, L28
- Ellingsen, S. P., Chen, X., Breen, S. L., & Qiao, H.-H. 2017a, *MNRAS*, 472, 604
- Ellingsen, S. P., Chen, X., Breen, S. L., & Qiao, H.-H. 2017b, *ApJ*, 841, L14
- Galametz, M., Zhang, Z.-Y., Immer, K., et al. 2016, *MNRAS*, 462, L36
- Gao, F., Braatz, J. A., Reid, M. J., et al. 2016, *ApJ*, 817, 128
- Gao, F., Braatz, J. A., Reid, M. J., et al. 2017, *ApJ*, 834, 52
- Gardner, F. F. & Whiteoak, J. B. 1975, *MNRAS*, 173, 77p
- Ginsburg, A., Walsh, A., Henkel, C., et al. 2015, *A&A* 584, L7
- Greene, J. E., Peng, C. Y., Kim, M. et al. 2010, *ApJ*, 721, 26
- Greene, J. E., Seth, A., den Brok, M., et al. 2013, *ApJ*, 771, 121
- Greene, J. E., Seth, A., Kim, M., et al. 2016, *ApJ*, 826, L32
- Greenhill, L. J., Henkel, C., Becker, R., Wilson, T.L., Wouterloot, J. G. A. 1995, *A&A*, 304, 21
- Hagiwara, Y., Doi, A., & Hachisuka, K. 2013a, *ASP Conf. Ser.*, 476, 295
- Hagiwara, Y., Miyoshi, M., Doi, A., & Horiuchi, S. 2013b, *ApJ*, 768, L38
- Hagiwara, Y., Horiuchi, S., Doi, A., Miyoshi, M., & Edwards, P. G. 2016, *ApJ*, 827, 69
- Haschick, A. D., Baan, W. A., & Peng, E. W. 1994, *ApJ*, 437, L35
- Henkel, C., Wang, Y. P., Falcke, H., Wilson, A. S., Braatz, J. A. 1998, *A&A*, 335, 463
- Henkel, C., Peck, A. B., Tarchi, A., et al. 2005, *A&A*, 436, 75
- Henkel, C., Braatz, J. A., Reid, M. J., et al. 2012, *IAUS*, 336, 301
- Herrnstein, J. R., Moran, J. M., Greenhill, L. J., et al. 1999, *Nature*, 400, 539
- Humphreys, E. M. L., Greenhill, L. J., Reid, M. J. 2005, *ApJ*, 634, L133
- Humphreys, E. M. L., Vlemmings, W. H. T., Impellizzeri, C. M. V., et al. 2016, *A&A*, 592, L13
- Imai, H., Katayama, Y., Ellingsen, S. P., & Hagiwara, Y. 2013, *PASJ*, 65, 28
- Impellizzeri, C. M. V., McKean, J. P., Castangia, P., et al. 2008, *Nature*, 456, 927
- Johanson, A. K., Migenes, V., & Breen, S. L. 2014, *ApJ*, 781, 78
- Kamali, F., Henkel, C., Brunthaler, A., et al. 2017, *A&A*, 605, A84
- Kennicutt, R. C. 1998, *ARAA*, 36, 189
- König, S., Eckart, A., Henkel, C., & García-Marín, M. 2012, *MNRAS*, 420, 2263
- Kuo, C. Y., Braatz, J. A., Condon, J. J., et al. 2011, *ApJ*, 727, 20
- Kuo, C. Y., Braatz, J. A., Reid, M. J., et al. 2013, *ApJ*, 767, 154
- Kuo, C. Y., Braatz, J. A., Lo, K. Y., et al. 2015, *ApJ*, 800, 26
- Kylafis, N. D., & Norman, C. A. 1991, *ApJ*, 373, 525
- Läsker, R., Greene, J. E., Seth, A., et al. 2016, *ApJ*, 825, 3

- Liu, Z. W., Zhang, J. S., Henkel, C., et al. 2017, *MNRAS*, 466, 1608
- Mangum, J. G., Darling, J., Menten, K. M., & Henkel, C. 2008, *ApJ*, 673, 832
- Mangum, J. G., Darling, J., Henkel, C. & Menten, K. M. 2013, *ApJ*, 766, 108
- Maoz, E., & McKee, C. F. 1998, *ApJ*, 494, 218
- Matsushita, S., Trung, D.-V., Boone, F., et al. 2015, *ApJ*, 799, 26
- McCarthy, T. P., Ellingsen, S. P., Chen, X., et al. 2017, *ApJ*, 846, 156
- McKean, J. P., Impellizzeri, C. M. V., Roy, A. L., et al. 2011, *MNRAS*, 410, 2506
- Menten, K. M. 1991, *ApJ*, 380, L75
- Miyoshi, M., Moran, J., Herrnstein, J., et al. 1995, *Nature*, 373, 127
- Nakai, N., Inoue, M., & Miyoshi, M. 1993, *Nature*, 361, 45
- Pesce, D. W., Braatz, J. A., Condon, J. J., et al. 2015, *ApJ*, 810, 65
- Pesce, D. W., Braatz, J. A., & Impellizzeri, C. M. V. 2016, *ApJ*, 827, 68
- Pjanka, P., Greene, J. E., Seth, A. C., et al. 2017, *ApJ*, 844, 165
- Reid, M. J., Braatz, J. A., Condon, J. J., et al. 2009 *ApJ*, 695, 287
- Reid, M. J., Braatz, J. A., Condon, J. J., et al. 2013, *ApJ*, 767, 154
- Scalise, E., & Braz, M. A. 1982, *A&A*, 87, 528
- Sjouwerman, L. O., Murray, C. E., Pihlström, Y. M., Fish, V. L., & Araya, E. D. 2010, *ApJ*, 724, 158
- Tarchi, A., Henkel, C., Chiaberge, M., & Menten, K. M. 2003, *A&A*, 407, L33
- Tarchi, A., Castangia, P., Columbano, A., Panessa, F., & Braatz, J. A. 2011, *A&A*, 532, A125
- van den Bosch, R. C. E., Greene, J. E., Braatz, J. A., Constantin, A., & Kuo, C.-Y. 2016, *MNRAS*, 455, 158
- Wagner, J. 2013, *A&A*, 560, A12
- Wiggins, B. K., Migenes, V., & Smidt, J. M. 2016, *ApJ*, 816, 55
- Yamauchi, A., Miyamoto, Y., Nakai, N., et al. 2017, *PASJ*, 69, L6
- Zhang, J. S., Henkel, C., Guo, Q., & Wang, J. 2012, *A&A*, 538, A152
- Zhang, J. S., Liu, Z. W., Henkel, C., Wang, J. Z., & Coldwell, G. V. 2017, *ApJ*, 836, L20
- Zschaechner, L. K., Ott, J., Walter, F., et al. 2016, *ApJ*, 833, 41